

# Versatile Colorant Syntheses by Multiple Condensations of Acetyl Anilines with Perylene Anhydrides\*\*

Daniel Jänsch, Chen Li, Long Chen, Manfred Wagner, and Klaus Müllen\*

Dedicated to Professor Wolfgang Lüttke on the occasion of his 95th birthday

**Abstract:** We report a key step forward in rylene chemistry: the transformation of rylene anhydrides into novel chromophore families. The imidization of rylene anhydrides with 2-acetyl anilines could be controlled by the choice of the solvent, thus causing a transformation into either a 4-hydroxyquinoline (4-HQ) or a 4-oxoquinoline (4-OQ) unit. The 4-OQ motif contains an aminoenone group formed by intramolecular aldol condensation and is the first vinylogous rylene imide. The concept of vinylogy was further developed by utilizing 2,6-diacetyl aniline leading to an 3a-aza-1,6-phenalenedione-extended rylene skeleton fully embracing the nitrogen atom. By functionalization of the aminoenone motifs, for example, malononitrile addition at the carbonyl groups, the optical and electronic properties could be further tuned.

**P**erylene-3,4:9,10-tetracarboxylic dianhydrides and their corresponding diimides (PDAs and PDIs) represent classical structure types of colorants and have found tremendous interest in fundamental and industrial research (Figure 1).<sup>[1]</sup> This attention has been further increased by their use in self-assembly studies<sup>[2]</sup> and by their role as active components of electronic<sup>[3]</sup> and optoelectronic devices.<sup>[4]</sup> Since the invention of PDI pigments by Kardos,<sup>[5]</sup> this chromophore has been investigated for more than 100 years. Quite naturally, many attempts have been undertaken to structurally modify PDAs and PDIs to control, for example, the wavelength of absorption and emission as well as the semiconducting properties. These include substitutions (Figure 1): a) at the imide nitrogen,<sup>[6]</sup> for example, leading to perylene tetracarboxylic bis(benzimidazole) (PTCBI)<sup>[7]</sup> or at the aromatic core<sup>[8]</sup> or b) enlargement of the perylene core towards terrylene,<sup>[9]</sup> quaterylene,<sup>[10]</sup> and even higher  $\pi$ -systems.<sup>[11]</sup>

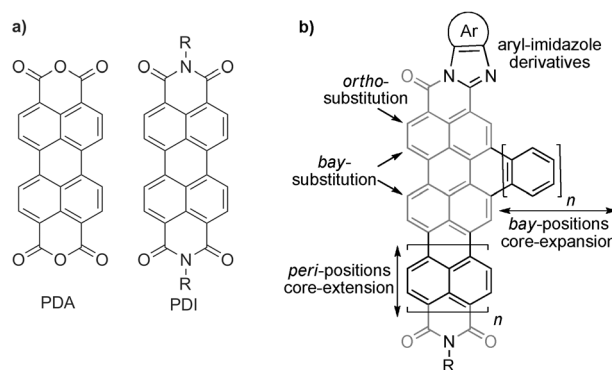


**Figure 1.** a) Structures of PDA and PDIs; b) schematic illustration of functionalization strategies.

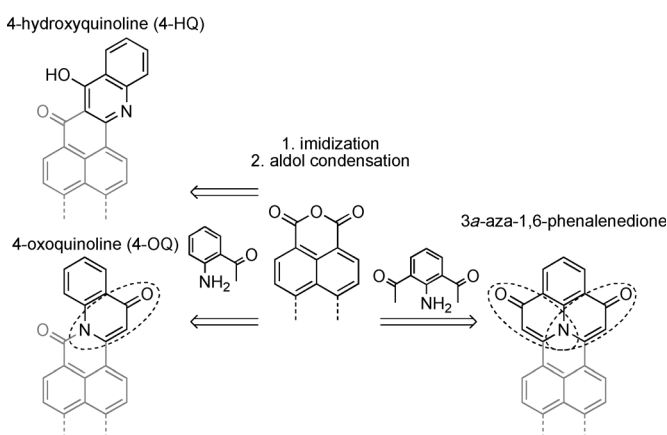


**Figure 2.** Concept for extension of the  $\pi$ -system; structural motifs of new chromophore families; vinylogous imide groups (dotted circles).

[\*] D. Jänsch, Dr. C. Li, Dr. L. Chen, Dr. M. Wagner, Prof. Dr. K. Müllen  
Max-Planck-Institut für Polymerforschung  
Ackermannweg 10, 55128 Mainz (Germany)  
E-mail: muellen@mpip-mainz.mpg.de

Dr. L. Chen  
Department of Chemistry, School of Science, Tianjin University  
300072 Tianjin (P. R. China)

[\*\*] We gratefully acknowledge financial support from BASF SE and cordially thank Dr. Dieter Schollmeyer for X-ray crystal structure analysis, Beate Müller for HPLC analytics, Dr. Henrike Wonneberger and Dr. Joseph Krumpfer who assisted in proofreading, and Dr. Yulian Zagaryanski for fruitful discussions.

Supporting information for this article is available on the WWW under <http://dx.doi.org/10.1002/anie.201409634>.

Herein, we introduce an elegant, but powerful concept for unprecedented extensions of the rylene skeleton, which comprises imidization of rylene anhydrides with acetyl-substituted anilines and subsequent intramolecular aldol condensation (Figure 2). We developed a procedure to selectively control the entry to novel chromophore families by the reaction of 2-acetyl anilines with rylene anhydrides. This was either directed towards 4-hydroxyquinoline (4-HQ) or 4-oxoquinoline (4-OQ) extended rylene skeletons (Figure 2).

As a consequence the 4-OQ-extended rylene skeletons can be regarded as heterocyclic benzantrones and violantrones

rather than derivatives of rylene imides.<sup>[12]</sup> The proximity of the hydroxy and carbonyl groups causes stabilizing hydrogen bonds and keto-enol tautomerism. The aminoenone moiety of the new six-membered ring in the 4-HQ motif represents a vinylogue of the dicarboximide structure. The conjugated system could be further extended by treating 2,6-diacetyl aniline with anhydrides forming an 3*a*-aza-1,6-phenalenedione unit with two aminoenone moieties fully embracing the nitrogen atom (Figure 2).

Encouraged by the reported condensation of 2-acetyl aniline with various acid anhydrides<sup>[13]</sup> we explored a model reaction with naphthalene monoanhydride (NMA). Most of the typical conditions for imidization reactions were found to be insufficient. Using imidazole as the solvent was not only the most efficient method for imidization, but also promoted the subsequent aldol condensation step. Surprisingly, the <sup>1</sup>H NMR and X-ray crystal-structure analysis of the isolated product revealed that it was not the expected vinylogous benzo[4,5]isoquinolino[2,1-*a*]quinoline-7,13-dione (**1**) but its structural isomer, 8-hydroxy-7*H*-naphtho[1,8-*bc*]acridin-7-one (**2**; Scheme 1).

For the synthesis of **1**, a three-step approach comprising imidization of NMA with 2-bromo aniline, acylation of **3** by a Stille coupling with tributyl(1-ethoxyvinyl)tin, and aldol condensation of the acetyl group with the imide carbonyl group was employed. When imidazole was utilized as the condensation agent, the 4-HQ-derivative **2** was obtained in

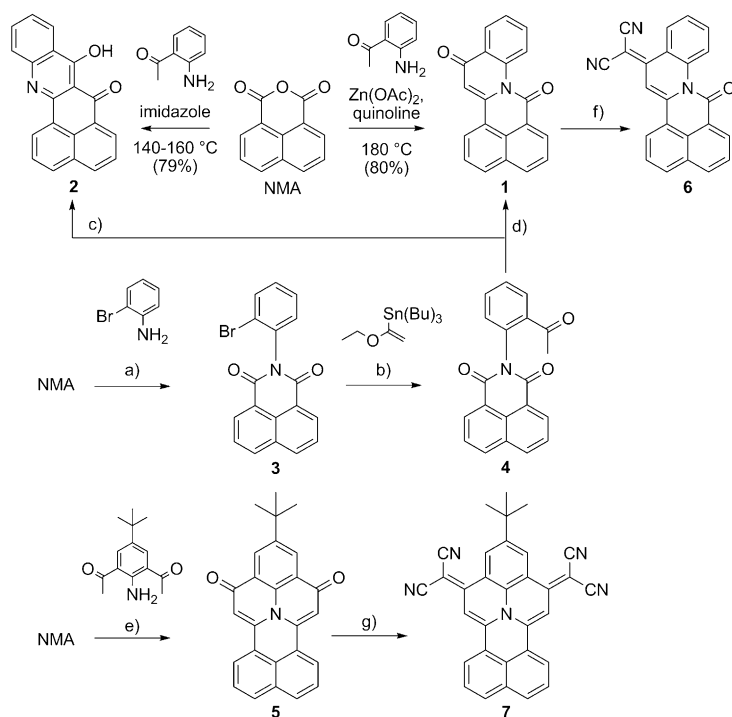
93% yield. However, when using quinoline as solvent under addition of catalytic amounts of zinc acetate, the reaction selectively generated the 4-OQ chromophore **1** starting from **4** in 82% yield. By the reaction of NMA with 2-acetyl aniline in quinoline, **1** was attained in 80% yield in a one-pot approach (Scheme 1).

The influence of imidazole on the course of the reaction was studied in detail by HPLC analysis and NMR spectroscopy after different reaction times (Figure S7 and S9 in the Supporting Information). The reaction proceeded by a fast imidization to form **4**. The aldol condensation towards **1** started within the first hour accompanied with a rearrangement reaction of **1** to **2**. The rearrangement process could be verified by the treatment of the vinylogous naphthalene monoimide (NMI) **1** with imidazole, which also resulted in the formation of **2** (Figure S8). In sharp contrast, only traces of **2** were observed at elevated temperatures and after addition of zinc acetate when quinoline was used as the solvent. We ascribe the different outcome of the imidization to the nucleophilic nature of imidazole, which can attack the amide bond of **1** and serve as leaving group during re-closure to the thermodynamically more stable isomer **2**. This stability arises from an additionally formed aromatic ring and intramolecular hydrogen bonds (Figure S2).

The elaborated reaction conditions were further applied for the condensation of NMA with 2,6-diacetyl-4-*tert*-butyl aniline to afford **5** in 25% yield. The yield of **5** increased to 52% when a threefold excess of NMA was employed. Using quinoline instead of imidazole led to longer reaction times without improving the yields (49%).

To evaluate the reactivity of the vinylogous aminoenone carbonyl groups towards olefination reactions, **1** and **5** were treated with malononitrile. With two and ten equivalents malononitrile only the aminoenone group of **1** underwent a Knoevenagel condensation, while the amide remained unreacted and **6** could be isolated in 31% and 42% yield, respectively. Its identity was confirmed by two-dimensional NMR spectroscopy. Both carbonyl groups of **5** react with malononitrile to form **7** as shiny deep violet crystals in 41% yield. In comparison to an imide carbonyl, the enonamine carbonyl group can more easily undergo olefination reactions.

The effects of the different extensions on the optical and electronic properties were studied and compared with those of 2,5-di-*tert*-butylphenylnaphthalene monoimide (**A**).<sup>[14]</sup> The enlargement of the conjugated system of the 4-OQ-naphthalene **1** results in a bathochromic shift of 57 nm ( $\epsilon_{(\lambda_{392})} = 19100 \text{ M}^{-1} \text{ cm}^{-1}$ ) towards **A** (Figure 3). Rearrangement and aromatization of **1** affording the 4-HQ-naphthalene **2** causes an even more red-shifted absorption maximum at  $\lambda_{\text{max}} = 425 \text{ nm}$ . The incorporation of the nitrogen atom into the 3*a*-aza-1,6-phenalenedione motif leads to an absorption maximum of **5** at  $\lambda_{\text{max}} = 415 \text{ nm}$  with a strong red-shift (80 nm) in comparison to **A**. Attributed to the



**Scheme 1.** Synthesis of vinylogous NMI **1** and its 4-HQ isomer **2**, vinylogous NMI **5** and olefination products with malononitrile **6** and **7**: a) quinoline,  $\text{Zn}(\text{OAc})_2$ , 180 °C, 16 h, 84%; b) 1.  $[\text{Pd}(\text{PPh}_3)_4]$ , toluene, 110 °C, 18 h, 2. 2 M  $\text{HCl}_{\text{aq}}$ , 72%; c) imidazole, 140 °C, 6 h, 93%; d) quinoline,  $\text{Zn}(\text{OAc})_2$ , 180 °C, 24 h, 82%; e)  $\text{Zn}(\text{OAc})_2$ , base, 140–180 °C, 10–52%; f)  $\text{AcOH}$ ,  $\text{Ac}_2\text{O}$ , malononitrile, reflux, 31%; g)  $\text{AcOH}$ ,  $\text{Ac}_2\text{O}$ , malononitrile, reflux, 41%.

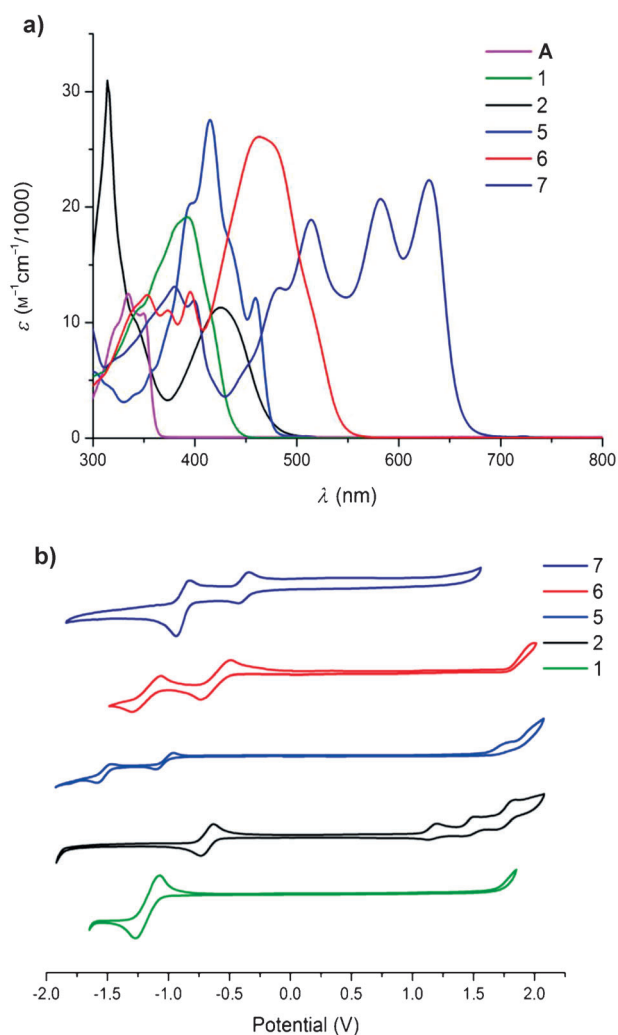


**Figure 3.** Absorption spectra of **1** (green), **2** (black), **5** (blue), **6** (red), **7** (cyan) and 2,5-di-*tert*-butylphenyl-NMI (**A**; magenta) in  $\text{CH}_2\text{Cl}_2$  ( $10^{-5}$  M); Cyclic voltammograms of compounds **1** (green), **2** (black), **5** (blue), **6** (red) and **7** (cyan) at a scan rate of  $0.1 \text{ V s}^{-1}$ .

extended  $\pi$ -system, the molar absorption coefficient is twice as high ( $\epsilon_{(\lambda 415)} = 27000 \text{ M}^{-1} \text{ cm}^{-1}$ ) as **A** ( $\epsilon_{(\lambda 335)} = 12500 \text{ M}^{-1} \text{ cm}^{-1}$ ), and **2** ( $\epsilon_{(\lambda 425)} = 11300 \text{ M}^{-1} \text{ cm}^{-1}$ ). The absorption spectrum of the malononitrile adducts **6** and **7** reveal four absorption bands in a broad range from 430–660 nm.

The energy levels of the molecular orbitals of **1**, **2**, **5**, **6**, and **7** were investigated by cyclic voltammetry. The photophysical and electrochemical data and HOMO and LUMO levels are summarized in Table 1. The LUMO energy levels of  $-3.34$  and  $-3.42 \text{ eV}$  for **2** and **5**, respectively, indicated a weak electron affinity. The condensation with malononitrile led to lower LUMO energy levels of  $-3.68$  and  $-4.11 \text{ eV}$  for **6** and **7**, respectively, indicating their suitability as n-type semiconductors.

X-ray single-crystal analysis of **7** revealed that the 3*a*-aza-1,6-phenalenedione motif is fairly planar, but slightly twisted towards the naphthalene unit by  $12\text{--}15^\circ$  (Figure 4). The intermolecular distance of approximately  $3.5 \text{ \AA}$  suggested weak interactions.

**Table 1:** Optical and electronic properties of compounds **1**, **2** and **5–7**.

Comp.	$\lambda$ [nm] <sup>[a]</sup>	$\epsilon$ [ $\text{M}^{-1} \text{ cm}^{-1}$ ]	$E_{\text{red}}^{[b]}$ [V]	$E_{\text{ox}}^{[b]}$ [V]	$E_{\text{g}}^{[c]}$ [eV]	$E_{\text{LUMO}}^{[d]}$ [eV]	$E_{\text{HOMO}}^{[e]}$ [eV]
<b>1</b>	392	19100	$-1.07$	–	2.85	$-3.34$	$-6.18^{[f]}$
<b>2</b>	425	11300	$-0.59$	1.10	2.63	$-3.81$	$-5.50$
<b>5</b>	415	27000	$-0.92$	1.60	2.62	$-3.48$	$-6.00$
<b>6</b>	463	26100	$-0.72$	–	2.25	$-3.68$	$-5.93^{[f]}$
<b>7</b>	630	23200	$-0.32$	–	1.89	$-4.08$	$-5.97^{[f]}$

[a] UV/Vis absorption maximum in the visible region in  $\text{CH}_2\text{Cl}_2$ .

[b] Determined by cyclic voltammetric measurement in  $0.1 \text{ M}$  solution of  $\text{Bu}_4\text{NPF}_6$  in  $\text{CH}_2\text{Cl}_2$  with a scan rate of  $0.1 \text{ V s}^{-1}$ . [c] Optical gap energy  $E_{\text{g}} = 1240/\lambda_{\text{onset}}$ ;  $\lambda_{\text{onset}}$  estimated from the onset of the longest wavelength of corresponding absorption spectra. [d] Estimated versus vacuum level from  $E_{\text{LUMO}} = -4.80 \text{ eV} - (E_{\text{red}} - E_{\text{Fc}})$ . [e] Estimated versus vacuum level from  $E_{\text{HOMO}} = -4.80 \text{ eV} - (E_{\text{ox}} - E_{\text{Fc}})$ . [f] Calculated from the optical gap energy  $E_{\text{g}}$  using the equation  $E_{\text{HOMO}} = E_{\text{LUMO}} - E_{\text{g}}$ .

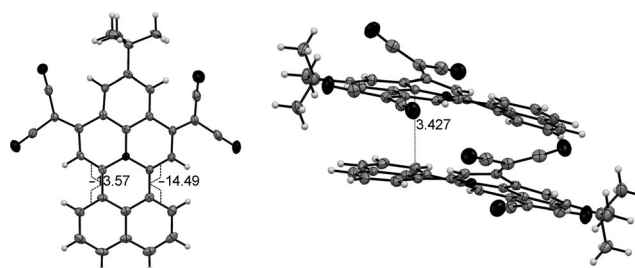


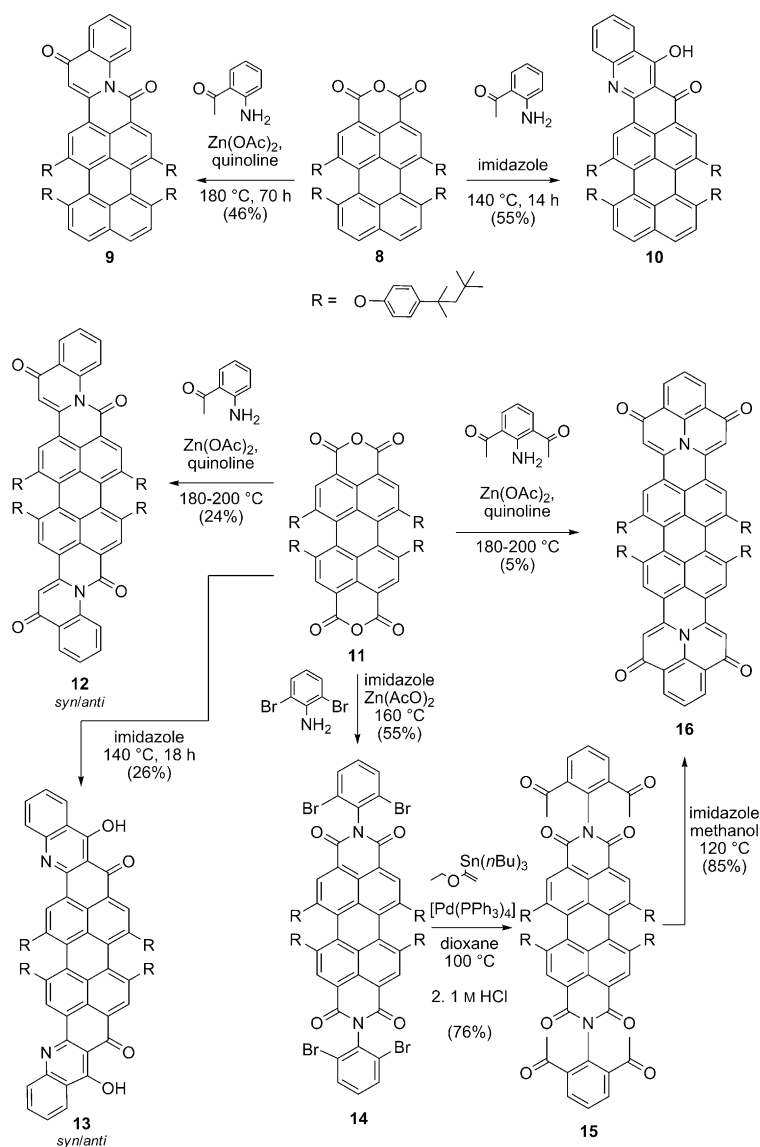
**Figure 4.** X-ray single-crystal analysis of **7** (thermal ellipsoids set at 50% probability, nitrogen atoms in black).left: torsion angle within **7**, right: packing in unit cell.

The tremendous effect of the novel structural moieties on the optical properties motivated us to further extend this concept towards perylene-based NIR-dyes. First, 2-acetyl aniline was reacted with tetra-*tert*-octylphenoxy perylene monoanhydride **8**. With quinoline as solvent and catalytic amounts of zinc acetate, compound **9** was isolated in 46% yield as a light purple solid. Its structural isomer **10** was obtained from an imidazole melt as a violet solid in 55% yield.

Treating the literature known tetra-*tert*-octylphenoxy-PDA (**11**)<sup>[15]</sup> with 2-acetyl aniline in quinoline with catalytic amounts of zinc acetate afforded the blue solid **12** as a mixture of *syn*- and *anti*-isomers in 24% yield. With imidazole as solvent, rearrangement took place to form the twofold 4-HQ extended perylene **13** as a green solid in 26% yield.

Direct condensation of 2,6-diacetyl aniline<sup>[16]</sup> with PDA **11** in quinoline with zinc acetate gave a complex reaction mixture and the target compound **16** could be isolated in a yield of only 5%. The low yields of this reaction could be explained by a) the low amine nucleophilicity, b) an auto-condensation of the acetyl anilines in a Friedländer reaction,<sup>[17]</sup> c) partial decarboxylation.<sup>[18]</sup> After numerous attempts to increase the yields, an alternative synthetic route for **12** with sequential imidization, acylation, and a final aldol condensation was developed (Scheme 2).

The reaction of PDA **11** with 2,6-dibromoaniline in imidazole led to PDI **14** in 55% yield. Then, the four



**Scheme 2.** Synthesis of the structural isomers **9** and **10**, vinylogous PDIs **12** and **16** and 4-hydroxyquinoline derivative **13**.

bromo-groups of **14** were transformed into acetyl groups by Stille coupling with tributyl(1-ethoxyvinyl)tin to obtain tetraacetylated PDI **15** in 76% yield. Heating of **15** in a mixture of methanol/imidazole (1:1) at 120 °C gave product **16** in 85% yield as a green solid.

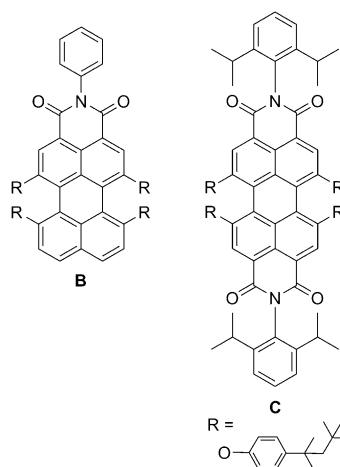
The absorption and emission spectra (Figure 5) of the 4-OQ-peryene **9** and 4-HQ-peryene **10** are compared with tetra-phenoxylated *N*-phenyl-peryene monoimide (**B**,  $\lambda_{\text{max}} = 544 \text{ nm}/\epsilon_{(\lambda,544)} = 28900 \text{ M}^{-1} \text{ cm}^{-1}$ ). The isomeric mixtures of **12** and **13** as well as doubly 3*a*-aza-1,6-phenalenedione-fused peryene **16** are collated with phenoxylated *N,N'*-diisopropylphenyl-PDI (**C**,  $\lambda_{\text{max}} = 582 \text{ nm}/\epsilon_{(\lambda,582)} = 55000 \text{ M}^{-1} \text{ cm}^{-1}$ ). Both series exhibit similar trends. The formation of 4-oxoquinoline motifs from anhydrides causes a bathochromic shift towards the respective imides of 23 and 50 nm for **9** ( $\lambda_{\text{max}} = 573 \text{ nm}/\epsilon_{(\lambda,573)} = 23300 \text{ M}^{-1} \text{ cm}^{-1}$ ) and **12** ( $\lambda_{\text{max}} = 633 \text{ nm}/\epsilon_{(\lambda,633)} = 62800 \text{ M}^{-1} \text{ cm}^{-1}$ ), respectively. Their structural isomers **10**

( $\lambda_{\text{max}} = 597 \text{ nm}/\epsilon_{(\lambda,597)} = 31100 \text{ M}^{-1} \text{ cm}^{-1}$ ) and **13** ( $\lambda_{\text{max}} = 662 \text{ nm}/\epsilon_{(\lambda,633)} = 57200 \text{ M}^{-1} \text{ cm}^{-1}$ ) reveal an additional shift towards longer wavelength absorption by 24 and 29 nm, respectively. Doubly 3*a*-aza-1,6-phenalenedione-fused peryene **16** demonstrates an absorption maximum at  $\lambda_{\text{max}} = 700 \text{ nm}$  with an absorption coefficient of  $\epsilon_{(\lambda,700)} = 69000 \text{ M}^{-1} \text{ cm}^{-1}$  and a distinct bathochromic shift of  $\Delta\lambda \approx 120 \text{ nm}$  compared to **C**, accompanied by an increase of the molar absorption coefficients.

The 4-HQ derivatives **3**, **10**, and **13** only exhibit a residual fluorescence in solution. This fluorescence quenching can be attributed to non-radiative deactivation via intramolecular hydrogen bonds, which involves keto–enol tautomerization.

The absorption spectra of **12** and **16** have rather similar vibrational structures, typical for perylene diimides (Figure 5c). The fluorescence spectra of **12** and **16** displays mirror symmetry between absorption and emission bands indicating that little structural rearrangement occurs between the ground and the excited state. Compound **12** is fluorescent at  $\lambda_{\text{em}} = 664 \text{ nm}$  with a Stokes shift of  $\Delta\lambda = 31 \text{ nm}$ , while **16** shows the emission maximum at  $\lambda_{\text{em}} = 726 \text{ nm}$  with a Stokes shift of  $\Delta\lambda = 26 \text{ nm}$ . The fluorescence quantum yield has been evaluated versus Rhodamine 800 as  $\Phi = 65\%$  for **12** and  $\Phi = 45\%$  for **16**. Thus, these compounds are valuable emitters in the range between visible and near infrared.

In conclusion, we have reported novel concepts for the synthesis of two new dyestuff families by a convenient synthetic scheme. The 4-HQ extended chromophores and the vinylogous rylene imides with one or two aminoenone moieties exhibit a strong shift of the absorption bands towards the NIR regime compared to their parent imides. Moreover, a fine-tuning of long-wavelength absorption from  $\lambda = 425$  to 660 nm was demonstrated by variation of the enoneamine carbonyl groups of the vinylogous naphthalene imides. Both





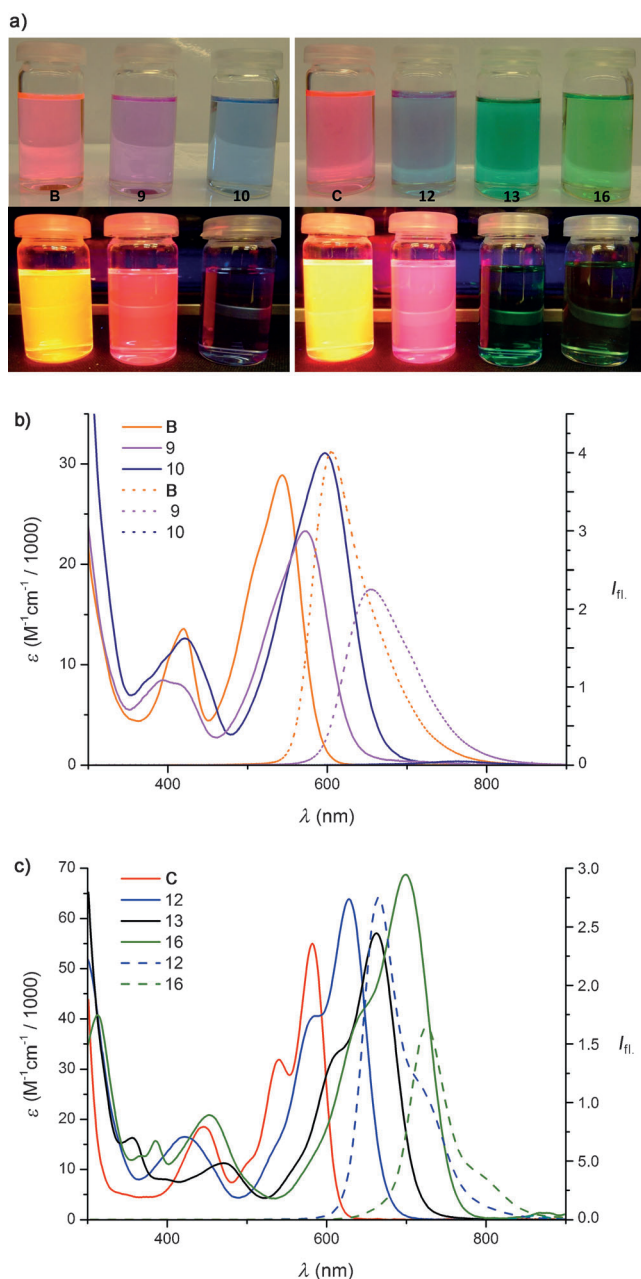


**Figure 5.** a) Photographs of **B**, **9**, **10**, **C**, **12**, **13**, and **16** in CH<sub>2</sub>Cl<sub>2</sub> under room light (top) and UV lamp (365 nm; bottom); b) Absorption spectra (solid lines) of **B** (orange), **9** (purple), and **10** (blue) in CH<sub>2</sub>Cl<sub>2</sub> (10<sup>-5</sup> M); emission spectra (dotted lines) of **B** (orange) and **9** (purple) in CH<sub>2</sub>Cl<sub>2</sub> (10<sup>-5</sup> M). c) Absorption spectra (solid lines) of **C** (red), **12** (blue), **13** (black), and **16** (green) and in CH<sub>2</sub>Cl<sub>2</sub> (10<sup>-5</sup> M); emission spectra (dotted lines) of **12** (blue) and **16** (green) in CH<sub>2</sub>Cl<sub>2</sub> (10<sup>-5</sup> M).

families hold promise as colorants and new materials for organic electronics.

Received: September 30, 2014

Published online: January 13, 2015

**Keywords:** aldol condensations · heterocyclic compounds · naphthalenes · perylenes · rearrangements

- [1] a) W. Herbst, K. Hunger, in *Industrial Organic Pigments*, 3rd ed., Wiley-VCH, Weinheim, **2006**; b) A. Herrmann, K. Müllen, *Chem. Lett.* **2006**, 35, 978–985.
- [2] F. Würthner, *Chem. Commun.* **2004**, 1564–1579.
- [3] C. Huang, S. Barlow, S. R. Marder, *J. Org. Chem.* **2011**, 76, 2386–2407.
- [4] a) C. W. Tang, *Appl. Phys. Lett.* **1986**, 48, 183–185; b) C. Li, H. Wonneberger, *Adv. Mater.* **2012**, 24, 613–636; c) A. Mishra, K. R. Fischer, P. Bäuerle, *Angew. Chem. Int. Ed.* **2009**, 48, 2474–2499; *Angew. Chem.* **2009**, 121, 2510–2536.
- [5] M. Kardos, Deutsches Reichspatent No. 276357, **1913**.
- [6] a) J. Feng, B. Liang, D. Wang, L. Xue, X. Li, *Org. Lett.* **2008**, 10, 4437–4440; b) K. J. Thorley, F. Würthner, *Org. Lett.* **2012**, 14, 6190–6193; c) N. Buffet, É. Grelet, H. Bock, *Chem. Eur. J.* **2010**, 16, 5549–5553; d) Y. Li, G. Zhang, G. Yang, Y. Guo, C. Di, X. Chen, Z. Ziu, H. Liu, Z. Xu, W. Xu, H. Fu, D. Zhang, *J. Org. Chem.* **2013**, 78, 2926–2934.
- [7] a) H. Quante, Y. Geerts, K. Müllen, *Chem. Mater.* **1997**, 9, 495–500; b) M. Mamada, P. Anzenbacher, *Org. Lett.* **2011**, 13, 4882–4885; c) M. Mamada, C. P. Bolívar, D. Kumaki, N. A. Esipenko, S. Tokito, P. Anzenbacher, *Chem. Eur. J.* **2014**, 20, 11835–11846.
- [8] a) C. Lütke Eversloh, C. Li, K. Müllen, *Org. Lett.* **2011**, 13, 4148–4150; b) W. Jiang, Y. Li, W. Yue, Y. Zhen, J. Qu, Z. Wang, *Org. Lett.* **2010**, 12, 228; c) S. Müller, K. Müllen, *Chem. Commun.* **2005**, 4045–4046; d) S. Alibert-Fouet, I. Seguy, J.-F. Bobo, P. Destruel, H. Bock, *Chem. Eur. J.* **2007**, 13, 1746–1753.
- [9] F. Holtrup, G. Müller, H. Quante, S. de Feyter, F. C. De Schryver, K. Müllen, *Chem. Eur. J.* **1997**, 3, 219–225.
- [10] H. Quante, K. Müllen, *Angew. Chem. Int. Ed. Engl.* **1995**, 34, 1323–1325; *Angew. Chem.* **1995**, 107, 1487–1489.
- [11] Z. Yuan, S.-L. Lee, L. Chen, C. Li, K. S. Mali, S. De Feyter, K. Müllen, *Chem. Eur. J.* **2013**, 19, 11842–11846.
- [12] a) H.-S. Bien, J. Stawitz, K. Wunderlich in *Anthraquinone Dyes and Intermediates. Ullmann's Encyclopedia of Industrial Chemistry*, Wiley-VCH, Weinheim, **2000**; b) T. Sawada, H. Ishii, Y. Aoyama, T. Ueda, J. Aoki, M. Takekawa, *Synth. Commun.* **2012**, 42, 784–793; c) D.-V. Tinh, M. Fischer, W. Stadlbauer, *J. Heterocycl. Chem.* **1996**, 33, 905–910; d) L. Li, C. S. B. Gomes, P. T. Gomes, T. Pedro, T. M. Duarte, *Synth. Commun.* **2008**, 38, 4415–4425.
- [13] H. Z. Alkhatlan, *J. Chem. Res. Synop.* **1992**, 260–261.
- [14] D. Gosztola, M. P. Niemczyk, W. Svec, A. S. Lukas, M. R. Wasielewski, *J. Phys. Chem. A* **2000**, 104, 6545–6551.
- [15] H. Quante, Ph. D. thesis, University of Mainz (Germany), **1995**.
- [16] D. M. McKinnon, J. Y. Wong, *Can. J. Chem.* **1971**, 49, 2018–2022.
- [17] a) P. Friedländer, *Ber. Dtsch. Chem. Ges.* **1882**, 15, 2572; b) J. Marco-Contelles, E. Pérez-Mayoral, A. Samadi, M. Carreiras, E. Soriano, *Chem. Rev.* **2009**, 109, 2652–2671.
- [18] a) A. Böhm, W. Helfer, DE 19501737, **1996**; b) M. Könnemann, P. Blaschka, H. Reichelt, DE 102004054303, **2006**; c) K. Tomizaki, P. Thamyongkit, R. S. Loewe, J. S. Lindsey, *Tetrahedron* **2003**, 59, 1191–1207.